Case Studies in Thermal Engineering 42 (2023) 102713

Contents lists available at ScienceDirect

Case Studies in Thermal Engineering

journal homepage: www.elsevier.com/locate/csite

Estimation of heat transfer parameters of shell and helically coiled tube heat exchangers by machine learning

Andaç Batur Çolak [a,*], Dogan Akgul [b,c], Hatice Mercan [d], Ahmet Selim Dalkılıç [c], Somchai Wongwises [e,f]

[a] Information Technologies Application and Research Center, Istanbul Commerce University, Istanbul 34445, Türkiye
[b] Department of Mechanical Engineering, Faculty of Engineering and Architecture, Istanbul Nisantasi University, Istanbul 34398, Türkiye
[c] Department of Mechanical Engineering, Mechanical Engineering Faculty, Yildiz Technical University (YTU), Istanbul 34349, Türkiye
[d] Department of Mechatronics Engineering, Faculty of Mechanical Engineering, Yildiz Technical University (YTU), Istanbul 34349, Türkiye
[e] Department of Mechanical Engineering, Faculty of Engineering, King Mongkut's University of Technology Thonburi (KMUTT), Bangkok 10140, Thailand
[f] National Science and Technology Development Agency (NSTDA), Pathum Thani 12120, Thailand

ARTICLE INFO

Keywords:
ANN
MLP
Levenberg-Marquardt
Heat exchanger
Helically coiled tube

ABSTRACT

Shell and helically coiled tube heat exchangers (SHCTHEXs) are heat exchangers that only take up a small space and enable greater heat transfer area compared to traditional models. Information on 21 different SHCTHEXs obtained from catalog was considered for the modeling. Two other artificial neural network structures have been created to forecast the heat transfer coefficient, pressure drop, Nusselt number, and performance evaluation criteria values as outputs. In contrast, tubing and coil diameters, Reynolds and Dean numbers, curvature ratio, and mass flow rate are designed as inputs. In the network structures with 105 data points, 70% of the data was used for training, 15% for validation, and 15% for the testing stages. The Levenberg-Marquardt procedure was evaluated as the training algorithm in multi-layer perceptron network models. The coefficient of determination was as higher than 0.99. The mean deviation was less than 0.01%. The results show that the created artificial neural network structures can acqurately estimate the outputs.

1. Introduction

A heat exchanger (HEX) is thermal equipment that transfers heat between fluids at different temperatures. Various procedures, which are categorized as active, passive, and compound, have been developed to enhance heat transfer (HT) in HEX [1]. With the decrease in conventional energy sources, the growing energy demands, and operating costs caused an investigation of better-performing small-sized HEXs, which operate using new-generation working fluids. The parametric and computational examinations have been accomplished to have the maximum efficiency in a shell and helically coiled tube heat exchanger (SHCTHEX) by researching optimum device dimensions and flow rates. The previous experimental and numerical studies showed that the SHCTHEX could perform better HT than straight tubular HEX [2–4]. Determination of optimal SHCTHEXs is a challenging task because the HT rates in HCT are greater than those in straight ones by secondary flow influences, but these effects lead to a more significant pressure drop (PD) compared to the straight tube. For that reason, HT rate and PD parameters should be considered together.

The theoretical and numerical analyses of HEX contain more assumptions and sophisticated correlations, but, the experimental

* Corresponding author.
E-mail address: abcolak@ticaret.edu.tr (A.B. Çolak).

https://doi.org/10.1016/j.csite.2023.102713
Received 8 November 2022; Received in revised form 28 December 2022; Accepted 4 January 2023
Available online 5 January 2023

works are pricey and time-consuming. To overcome these challenges, artificial neural network (ANN) analyses can be chosen for simulation, optimization, and performance estimation of HEXs [5], utilizing many data points belonging to the various pipe and coil diameters and mass flow rates. ANN is an artificial intelligence algorithm inspired by the idea of imitating the working of the human brain and occurred in the 1980s from developments in cognitive and computer science [6,7]. In addition, ANN does not require any particular equations or system setups. In the following paragraphs, some studies of ANN analyses for HEXs are mentioned briefly.

Beigzadeh and Rahimi [8] created ANN structures to predict HT and PD characteristics of 7 helical coils with various tube geometries. Four input parameters of the three-layer feed-forward ANN model, such as Reynolds number (Re) and Prandtl number (Pr), curvature ratio, and coil pitch. The model output were Nusselt number (Nu) and friction factor, and the results showed that the model gives accurate predictions of them in SHCTHEXs compared to computational and practical outcomes.

Cao et al. [9] examined the optimization of micro-finned HCTHEX in terms of HT, flow resistance, and entropy generation parameters. ANN models were created to approximate Nu, friction factor and entropy generation. The Re, pressure, coil diameter, and fin number were considered input parameters. The results of the developed ANN model were superior to the multiple linear regression ones, and finally, the most significant error was smaller than 8%.

Gill and Singh [10] experimentally investigated different-sized helically coiled capillary tubes in a refrigeration cycle with a mixture of R134a-LPG. After the study, they made an ANN structure to forecast the mass flow rate. The results revealed that the model prediction had high accuracy with experimental results and was better than the outcomes from the correlations. The absolute variance fracture is between 0.961 and 0.988. Additionally, the root means square error (RMSE) is between 0.489 and 0.275 kg/h and the mean absolute percentage error (MAPE) is between 4.75 and 2.31%.

Hajjat [11] introduced an ANN structure to guess the HT and flow dynamic mechanism of the shell and tube heat exchanger (STHEX). Al_2O_3/water and TiO_2/water nanofluids were chosen for working fluids. Input data of the simulation were Re, Pr, the volumetric nanofluid concentration and thermal conductivity. The researcher indicated that the ANN model prediction had sufficiently good results compared to experimental observation. The Nu and PD predictions were given by 9% and 9.6%, respectively.

Verma et al. [12] made an ANN analysis to estimate the HT performance of corrugated and smooth-surfaced tube HEX with different heights and pitches. They have obtained the highest heat transfer coefficient (HTC) and Nu for their HEX having 4 mm pitch and 1.5 mm depth helical-shaped ribs. The results indicated that the coefficients of multiple determinations are 0.99999 for Re, 0.999997 for HT, and 0.999993 for Nu. It is stated that the ANN technique has an excellent performance in predicting the performance of HEX.

Moya-Rico et al. [13] studied ANN structure to accurately estimate the HT and PD mechanisms in a triple pipe HEX with a corrugated and smooth surfaced inner tube. The model was developed by using more than 180 experimental datasets. The conclusion implied that the ANN showed accurate results compared to the experimental observation. The absolute mean relative deviation is lower than 1.91% and 3.82% for the HTC and PD, respectively.

Skrypnik et al. [14] created a new ANN model for predicting thermal and fluid dynamics performances in tubes with different-sized and shaped inner helical-finning under a turbulent flow regime. In their numerical investigation, they gathered empirical data from open sources to evaluate many datasets for the training stage of ANN structure. According to analysis, the MAPE values of 16.3% for *Nu* and 11.8% for friction factor. It is seen that the ANN structure predicts with good agreement compared to experiments.

Colak et al. [15] made ANN analyses to optimize and predict HT and PD parameters for double-tube HEXs. Two ANNs were evaluated using the multi-layer perceptron model. In the first model, 10 input parameters were defined, and in the second, 8 parameters were defined. The overall HTC, tube side and annulus side PD, and overall expenditure were predicted with deviations of 0.16%, 0.23%, 0.02%, and 0.003% by the first model, 0.02%, 0.18%, 0.16%, and 0.15% by the second one, respectively.

Devi et al. [16] conducted multi-layer perceptron (MLP)-ANN analysis using a feed-forward neural network with 3 layers to estimate Nu in double tube HEX with bare swirl tapes at altering swirl ratios. Re, Prandtl number and twist ratios were selected as input parameters, and numerical observations were evaluated using 33 empirical data. Consequently, the prediction of Nu has 90% accuracy, and the error rate is 0.01. The researchers suggested a model for the industry to examine the HT performance of HEXs with plain swirl tapes.

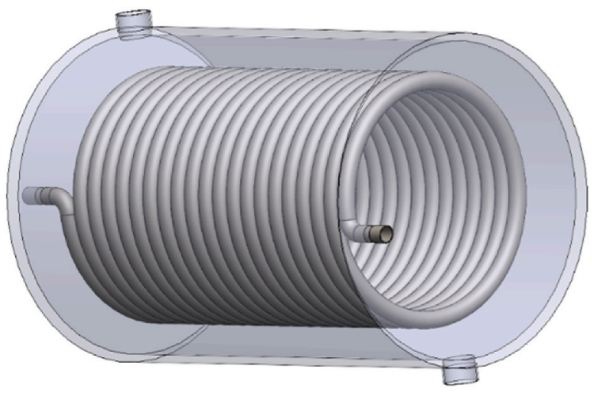

Fig. 1. Representation of the SHCTHEX [From Akgul et al. [18] with the permission from Springer].

Said et al. [17] did practical and computational work on the optimization of solar-powered STHEX. Multi-walled carbon nanotubes/water nanofluid with a concentration of 0.3% and 0.05% v was chosen as the operating fluid. MLP-ANN structure was employed to examine the performance of MWCNT/water and water on the tube and shell sides, in turn. The structure had a great regression coefficient and coefficient of determination for the pipe side as 0.998 and 0.996, while the shell side was 0.994 and 0.988, respectively.

The result from single-phase flow studies in SHCTHEXs shows the potential to merit research. There are quite a few studies that are not sufficient to neither explain the physics nor propose any practical correlation on the SHCTHEXs having enhanced surfaces. The current work can be used as an example for the estimation of heat transfer characteristics of SHCTHEXs shown in Fig. 1. Therefore, it should be one of the steps for researchers willing to examine the theoretical missing points of these HEXs. The proposed ANNs are considered to help predict varied HEX design factors with no extra parametric research. In the current investigation, the impacts of geometrical factors of pipe and coil diameters, and working conditions like Dean number (De) and Reynolds number (Re) on HT and PD in SHCTHEX are studied for laminar single-phase flow primarily at fixed heat flux. The performance evaluation criteria (PEC) technique is used for 21 dissimilar pipes with factors ranging from $1 < Pr < 3$, $1590 < Re < 11030$, $275 < De < 4680$. This work continue the authors' former parametrical study [18]. In the previous study, it was stressed that determining and working optimal velocity was one of the omitted problems of HEX calculations that affect initial and operational costs. Therefore, the pipe diameter is a significant input in the procedures regarding HT covering cost analyses. The primary purpose of the author's previous work was to remind the impact of various pure fluids and nanofluids on the optimal velocity affecting HT, pumping power, and expenditure, and to depict the most proper and cost-effective nanofluid for HEXs. In addition, PEC was reported to perform better prediction than the ε-NTU technique because the PEC definition contains Nu and the friction factor. Moreover, they highlighted the importance of laminar flows regarding PEC compared to turbulent flow in SHCTHEXs. Apart from Beigzadeh and Raimi [8], there is no other investigation about predicting HT characteristics of SHCTHEXs, according to the literature review above. The obtained results of the present study, as the second in the literature show, proposed ANN structures could accurately estimate the effects.

2. Calculation procedure

The study tested, 21 SHCHEXs with different tube and coil diameters. Various mass flow rates are applied on the tube side. A fixed flow rate is introduced on the shell side. Water is used as operating fluid on both sides. The alteration of Nu and PD with curvature diameter and the PD with tube diameter is shown in Fig. 2. The flow is always in a laminar regime with constant heat flux. The range of Pr is between 1 and 3, Re is between 1590-11030, and De is between 275-4680.

2.1. Determination of tube side Nusselt number

The chosen equation of curvature ratio [18], Re [19], De [20], and Nu [21] is shown in Eqs. (1)–(4), respectively.

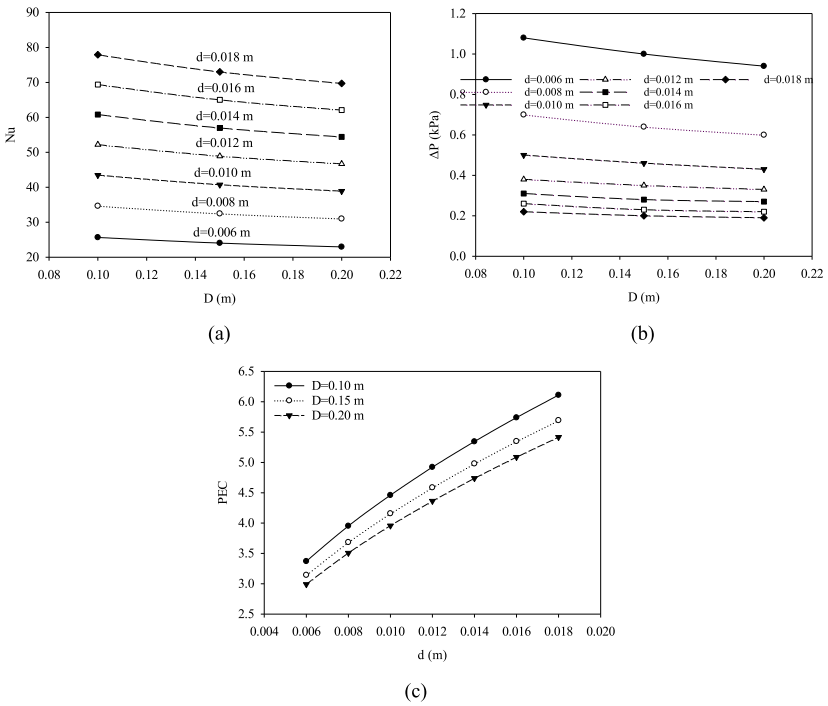

Fig. 2. The variation of Nusselt number with coil diameter (a), the pressure drops with coil diameter (b), and performance evaluation criteria with tube diameter (c) [From Akgul et al. [18] with permission from Springer].

$$\delta = \frac{d}{D} \tag{1}$$

$$Re = \frac{vd}{\nu} \tag{2}$$

$$De = Re\sqrt{\delta} \tag{3}$$

$$Nu = \left(0.76 + 0.65De^{0.5}\right)Pr^{0.175} \tag{4}$$

2.2. Determination of tube side convective heat transfer coefficient

The selected equations of the hydraulic diameter of the shell [22], inner and outer surface area of the tube, inner HTC [18], outer HTC [18] and overall HTC [19] are given in Eqs. (5)–(10), respectively.

$$D_{sh,h} = \frac{4\left[\left(\frac{\pi {D_{sh}}^2}{4}H_{sh}\right) - \left(\frac{\pi {d_o}^2}{4}L\right)\right]}{(\pi D_{sh}H_{sh}) + (\pi d_o L)} \tag{5}$$

$$A_{s,i} = \pi d_i L_t \tag{6}$$

$$A_{s,o} = \pi d_o L_t \tag{7}$$

$$h_i = \frac{Nuk}{d_i} \tag{8}$$

$$h_o = \frac{Nu_{sh}k}{d_o} \tag{9}$$

The shell side Nu is taken as 4.36 [19].

$$\frac{1}{UA_s} = \frac{1}{h_i A_{s,i}} + \frac{R_{fi}}{A_{s,i}} + \frac{\ln(d_o/d_i)}{2\pi k L_t} + \frac{R_{fo}}{A_{s,o}} + \frac{1}{h_o A_{s,o}} \tag{10}$$

For the temperature is low ($T < 50\ ^\circ C$) the fouling factor in the inner and outer side of the tube ($R_{f,i} = R_{f,o}$) are assumed as 0.0001 m^2K/W. For higher temperatures, they are assumed as 0.0002 m^2K/W [23,24].

2.3. Determination of tube side pressure drop

The selected equations of friction factors of the straight tube [19] and HCT [25] and pressure drop [19] are presented in Eqs. (11)–(13).

$$f_{st} = \frac{64}{Re} \tag{11}$$

$$\frac{f}{f_{st}} = \left[1 - \left(1 - \left(\frac{11.6}{De}\right)^{0.45}\right)^{\frac{1}{0.45}}\right]^{-1} \tag{12}$$

$$\Delta P = f\frac{L_t}{d_i}\frac{\rho v^2}{2} \tag{13}$$

2.4. Determination of performance evaluation criteria

The performance evaluation criterion may often be divided into two areas. One is that fluid characteristics are considered together with all affecting elements. This is often referred to as a "general method". In the first case, the generic techniques can be used as indications for thorough evaluations between heat transfer surfaces. This approach entails doing a rigorous heat exchanger or thermal analysis. It is incredibly challenging to draw a generalization that holds across a range of fluid characteristics. The alternative technique is based on assumptions, such as the constant thermophysical properties of fluids. The difference in the thermophysical properties is often not significant if the inlet temperatures are equal. The inaccuracies resulting from these assumptions are negligible for heat exchangers working with modest temperature variations [25].

The second method is more frequently used. The surface area may be calculated using the nominal or real surface area. The actual area of different structures is typically challenging to quantify, although the exact area of finned surfaces can be employed together with the additional area supplied by the fins. The unfinned surface's initial area serves as the foundation for the nominal area. This is a condensed strategy because all surfaces are contrasted with unaltered simple surfaces. The nominal area will be preferable if we compare the performance based on the same root surface. The reference surface might be a standard, enhanced or plain surface. Performance is often assessed at the same Re since enhanced, and referenced surfaces typically have a different flow rate for the same

pumping power and PD [26].

In the authors' previous parametric study [24], helical and straight tube HEX are compared under the same operating conditions and size. In the study, PEC is defined as [25].

$$PEC = \frac{(Nu/Nu_{st})}{(f/f_{st})^{1/3}} \tag{14}$$

In this present work, the same assumption is also used where the straight tube *Nu* is taken as 4.36 [19].

3. ANN model development

Two ANN structures have been developed to estimate the investigated HEX's dimensional and dimensionless HT characteristics. The initial ANN structure has dimensional inputs and outputs while the second has dimensionless ones. Therefore, ANN simulations have been performed to elucidate the effect of these indicated differences. MLP model, widely preferred with its strong architectural structures, is used in ANN models. MLP networks are structurally composed of three main layers, each directly associated with the next layer. The initial layer is the input layer, where data entry is made. The hidden layer is the after the input layer, and more than a single hidden layer can be introduced to an MLP algorithm. The estimated values are acquired in the output after the hidden layer. The first step in developing an MLP network model is identifying and optimizing the dataset. After the processes are performed, such as determining the data defined in the input layer, grouping the data set according to training, validation, and testing and, data is entered into the system. After determining the hyperparameters, such as the number of neurons, the training algorithm, the number of hidden layers, and the transfer function of the MLP network model, the training phase begins. Additionally, selecting the network model with the highest performance and lowest error rate signifies the training phase is finished. After determining the ideal MLP network model, the desired predictive values are obtained using the developed neural network. The flowchart of the development of an MLP neural network is given in Fig. 3. In the first model of MLP algorithms set in two different models, dimensional parameters (d, D, and m) have been introduced as input factors. The inner HTC and PD were calculated in the output one. In the second models of MLP algorithms, D and dimensionless parameters (Re_i, De, and δ) are defined as input parameters. Nu_i and PEC values are calculated in the output one. The symbolic pattern topology of the MLP algorithm is given in Fig. 4.

The model accuracy is predicted by optimizing and grouping the dataset in the ANN model. The data sets of both ANN models have been grouped in the structure with the greatest accuracy using the information obtained in the literature. A neuron is an element in the hidden one of the MLP algorithm. There is no fixed model or equation to find the number of neurons. This is one of the challenges of developing MLP algorithms. In the study, the MLP network performance is analyzed under different neuron numbers, which is an excepted and, thus, widely used method in the literature. Finally, 73 of the data used in the ANN structures developed with 105 data points have been gathered for training the structures, 16 for the validation phase, and 16 for testing. The fundamental structure of two dissimilar ANNs, which have various input and output factors and have created specific neuron numbers, is shown in Fig. 5.

The Levenberg-Marquardt training method is evaluated as the training one in this study. The Tan-Sig transfer function and output layer Purelin transfer function are used in the hidden layer. They are given as [27,28]:

$$f(x) = \frac{1}{1 + \exp(-x)} \tag{15}$$

$$\text{purelin}(x) = x \tag{16}$$

The terms used to evaluate the coefficient of determination (R) and mean squared error (MSE) values chosen as performance parameters are stated as [29,30]:

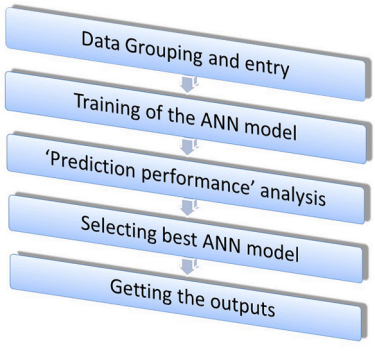

Fig. 3. The flowchart of the development stages of the MLP neural network.

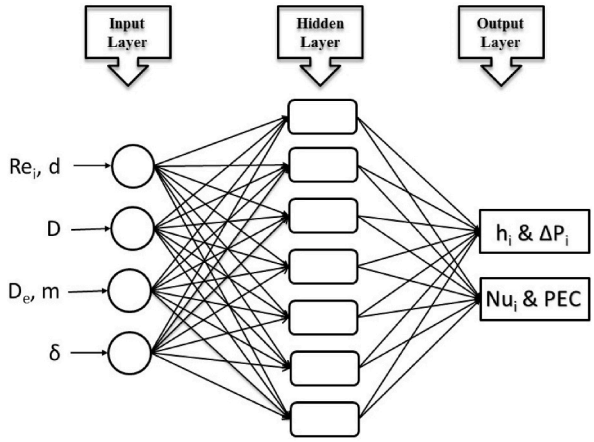

Fig. 4. The symbolic configuration topology of the MLP network model.

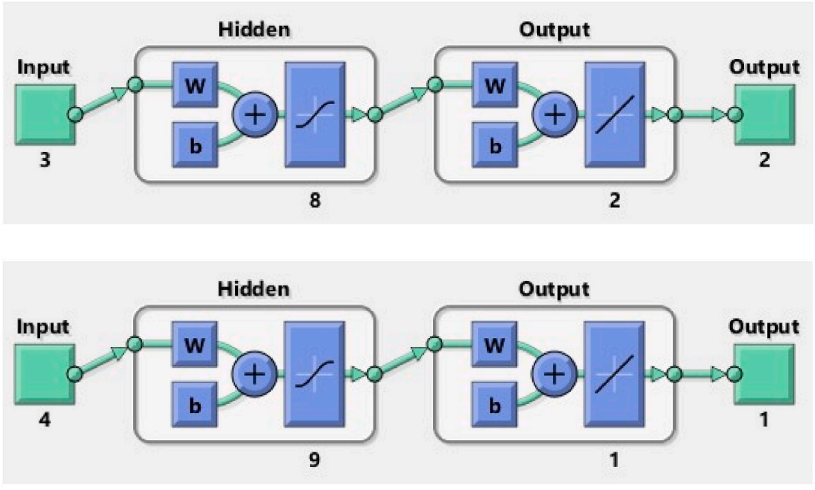

Fig. 5. The basic structure of two different ANN models.

$$R = \sqrt{1 - \frac{\sum_{i=1}^{N} \left(X_{targ(i)} - X_{ANN(i)}\right)^2}{\sum_{i=1}^{N} \left(X_{targ(i)}\right)^2}} \tag{17}$$

$$MSE = \frac{1}{N} \sum_{i=1}^{N} \left(X_{targ(i)} - X_{ANN(i)}\right)^2 \tag{18}$$

As another performance evaluation, the margin of deviation (MoD) values between the estimations gained from the ANN structures and the targets are calculated and analyzed comprehensively. The MoD values are calculated using [29,30]:

$$MoD = \left[\frac{X_{targ} - X_{ANN}}{X_{targ}}\right] x\ 100\ (\%) \tag{19}$$

4. Results and discussion

The problem in assessing HEXs is due to their methodological variety and the technical happenings for the period of the HT between the liquid or gas bodies. Primarily, each has been examined computationally, theoretically, and practically via the fundamentals of thermodynamics. Their analytical investigations contain more assumptions and complex equations. In addition, experimental works are expensive because of the initial investment required for building a setup. To correspond to these issues, ANNs were created to model, optimize, and forecast of HEXs' thermal characteristics. The suitable selection of a HEX is an onerousa duty for designers.

Principally, the remarkable parameter is accurately obtaining heating/cooling load. Next, additional factors are operating pressure, flow rate, and chemical coherence demands. Together with the HT, these components involve the arrangement and material. The main aim of the current study is to develop a computational simulation having 21 different SHCTHEXs for the simulation of the actual HEXs implementing the processes of MLP as favorable ANN choices.

In the first ANN, d, D, and m values were described as input factors, while the inner HTC and PD values were gained in the output layer. In the input layer of the second model, D, Re_i, De, and δ values were defined, while Nu_i and PECs were gained in the output layer. 73 of the data used in the ANN models, which were created with 105 data sets, were implemented for the training of the model, 16 for the validation, and 16 for the testing step. The number of neurons applied in the hidden layer of MLP networks has been optimized by determining the performances of different networks. In both MLPs, the Levenberg-Marquardt structure, one of the high-capability training ones, was used. The agreement of the estimated values acquired from the ANN with the targets was examined. It was found that the data were in ideal harmony.

The performance graph showing the MSE values acquired in the period of the training step is given in Fig. 6 to confirm the desired completion of the training phases of the MLP networks. In MLP networks, the data were sent back from the input to the output layer. The training cycle is restarted to reduce the differences between the predicted values acquired in the output one and the target data. Every process is named an "epoch". In Fig. 6, the MSEs, which were large in the training step of the MLP algorithm, reduce with the proceeding epochs. By the MSEs approaching the lowest value, the optimum performance was achieved, and the training step of MLP networks was completed. The proximity of MSEs to zero showed that the training phases of the developed MLP network models were perfectly terminated. Computed MSEs for the grouped data set of MLP algorithms are depicted in Table 1. The findings from Fig. 6 and Table 1 confirmed the successful completion of the training step of both MLP algorithm models developed.

The error histograms demonstrate the error values acquired during the training step of the ANN. The training accuracy could be examined by examining the errors gained throughout the training step of the structure. Fig. 7 shows the error histograms of both ANN models. When the error histograms were observed, the errors attained for the training, validation, and test data points were positioned quite near the nil error line. When the numerical values of the errors were considered, error values near to nil were obtained. The findings attained from the error histograms showed that the training step of both ANNs was completed with very low errors and ideal accuracy.

To inspect the prediction precision of the ANN, the compatibility of outputs and targets was examined. Fig. 8 shows the outputs and targets gained from the ANN for 4 different output parameters. The target and predicted values for all 4 output values were in good

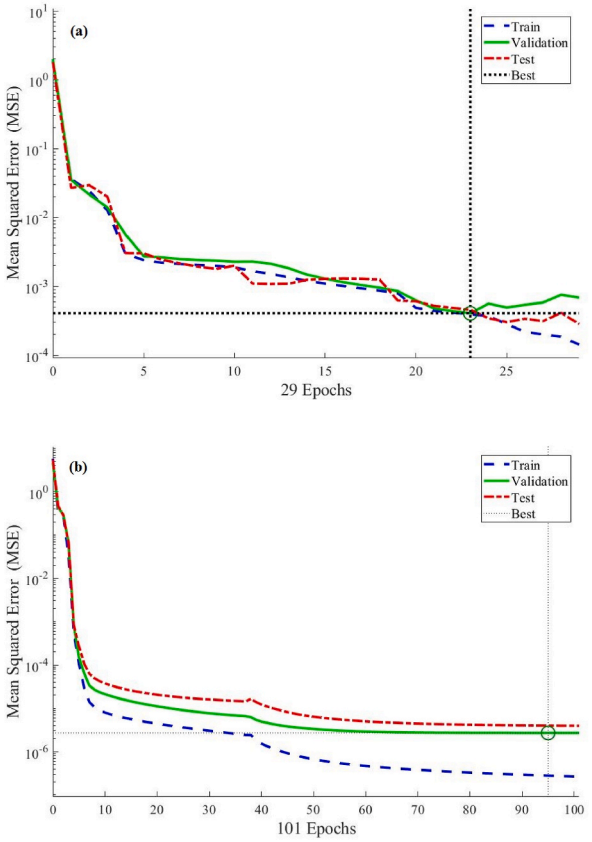

Fig. 6. Training performance of the MLP models.

Table 1
Performance results for the ANN models.

	Model 1		Model 2	
	MSE	R	MSE	R
Training	3.94E-04	0.99673	2.79E-07	0.99999
Validation	4.06E-04	0.99609	2.69E-06	0.99999
Test	4.56E-04	0.99816	3.99E-06	0.99999

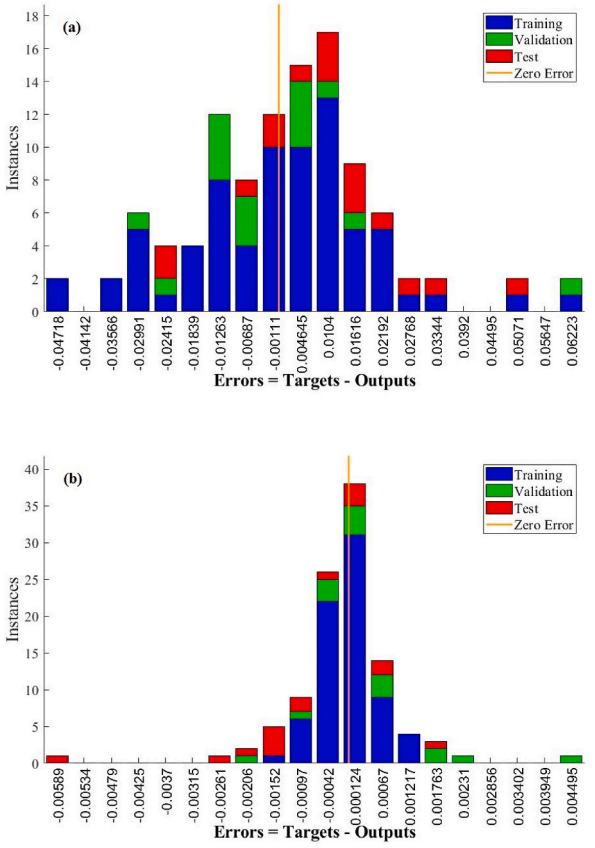

Fig. 7. Error histogram of the ANN models (a) Model 1 and (b) Model 2.

agreement. This good harmony of the data showed that both ANNs developed could predict and estimate inner HTC, PD, Nu_i, and PEC values with high precision.

It is significant to examine the MoDs that indicate the proportional deviation between the estimated inner HTC, PD, Nu_i, and PEC values and the targets. The MoDs computed for each of the 105 data sets used in the development of ANN models are shown in Fig. 9. The MoD values for every output were commonly concentrated around the nil deviation line. The nearness of the data sets indicating the MoDs to the nil deviation line expresses that the deviation rates between the forecast values attained from the ANN and the targets were small. The mean deviation values calculated for the estimated inner HTC, PD, Nu, and PEC values in the graphics were also lower than 0.01%. The consequences gained from the MoDs verified that both ANNs developed were created to make ideal estimation with quite low errors.

To perform a more detailed examination of the precision of the ANN models, the difference values between the targets and the ANN predictions at every data set were computed and illustrated in Fig. 10. The different values depicted for every output were quite low. The slight differences between the target values and the output ones obtained from the ANN showed that the forecast values gained from the ANN were close to the targets. Obtaining relatively low different values proved that the developed ANN could estimate inner HTC, PD, Nu, and PEC with relatively small errors.

While the target values of inner HTC, PD, Nu, and PEC parameters are on the abscissa of Fig. 11, the forecast values acquired from the ANN are on the ordinate. The locations of the data sets were generally placed above the nil error line. It should also be realized that the data sets obtained for each of the 4 output parameters were in the ±10% deviation lines. In Table 1, the calculated R values of three different data groups for both ANNs are above 0.99. These results show that both ANNs developed to provide very low errors and are

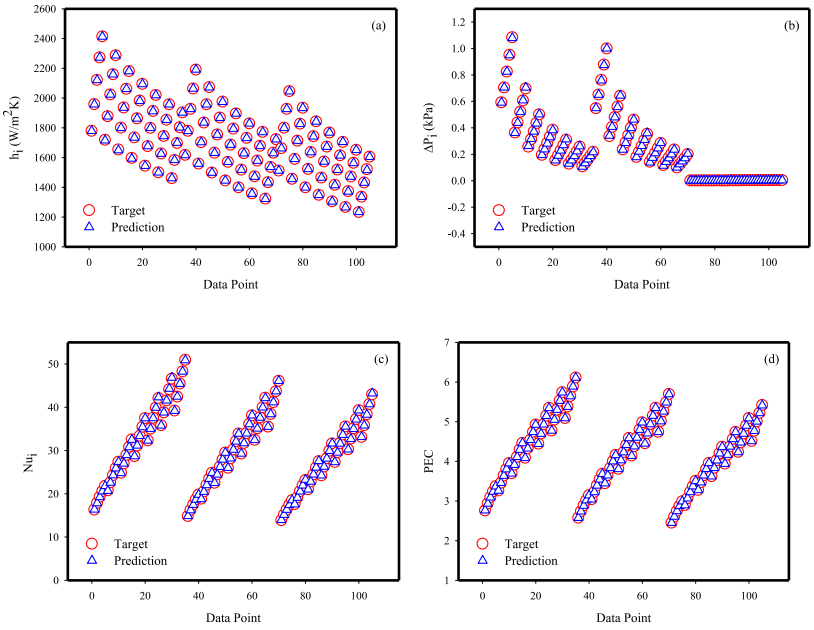

Fig. 8. The outputs and target values obtained from the ANN model for 4 different output parameters.

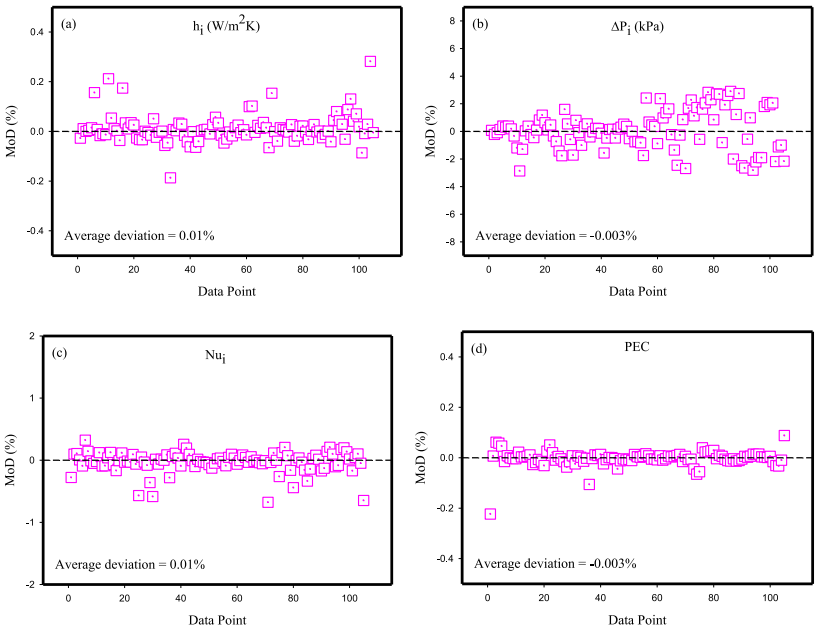

Fig. 9. MoD values according to data points for 4 different output parameters.

the best models that could be used to estimate inner HTC, PD, Nu, and PEC values.

5. Conclusion

The current investigation involves two different artificial neural network structures for determining the inner HTC, PD, Nu, and PEC values used as outputs. Tube and coil diameters, Re and De numbers, curvature ratio, and mass flow rate were inputs. A total of 21 different shell and helically coiled tube heat exchangers have been simulated as a new investigation from the most significant number of tested pipes reported in the literature. Therefore, designers are expected to benefit from the analyses as a preliminary parametric

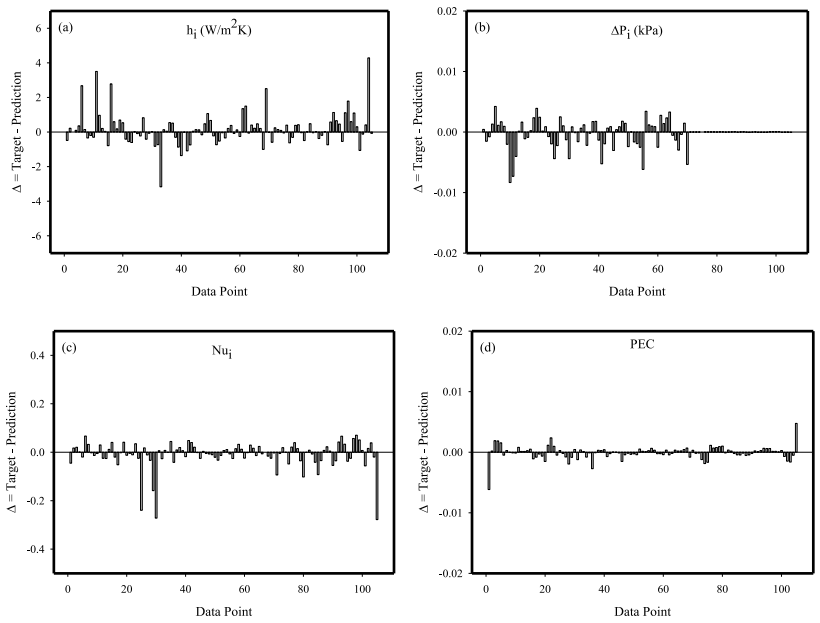

Fig. 10. The difference values between the target values and the ANN predictions at each data point.

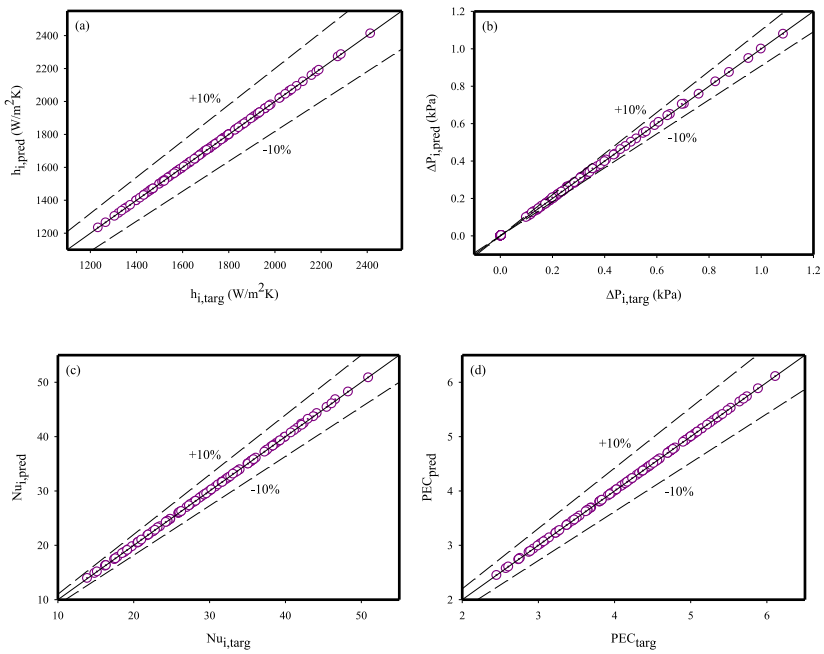

Fig. 11. The target data and ANN output 4 different output parameters.

step. After all, there is no other work on estimating heat transfer characteristics in shell and helically coiled tube heat exchangers. The results of the current study prove that the developed ANNs could accurately forecast the outputs. Consequently, the existing computational research should be evaluated as a sample for future investigations. The inner HTC, PD, Nu, and PEC values were predicted by creating two different ANNs. The MSEs selected as the prediction criteria were relatively low. The R-value, another prediction criterion, was computed as higher than 0.99. MoDs expressing the proportional deviation between target values and ANN outputs were found to be lower than 0.01%. The results obtained from ANN analyses show that they can predict the outputs with accurate precision. Therefore, ANNs are understood as the perfect engineering tool that could be used to estimate inner HTC, PD, Nu,

and PEC values.

Author statement

Andaç Batur Çolak: Conceptualization, software, writing - original draft. Dogan Akgul: Investigation, data curation, methodology. Hatice Mercan: Review. Ahmet Selim Dalkılıç: Supervision, project administration. Somchai Wongwises: Writing - review & editing, funding acquisition.

Declaration of competing interest

The authors declare that they have no known competing financial interests or personal relationships that could have appeared to influence the work reported in this paper.

Data availability

Data will be made available on request.

Acknowledgment

This work was supported by a grant from the Yildiz Technical University Coordinatorship of Scientific Research Projects, YTU-BAPK, and Project No: FOA-2019-3582. The fourth author acknowledges the visiting professorship from KMUTT. The fifth author acknowledges the NSTDA Research Chair Grant, and the Thailand Science Research and Innovation (TSRI) under Fundamental Fund 2023.

Nomenclature

c	capacity ratio
c_p	specific heat, kJ/kgK
d	tube inner diameter, m
D	coil diameter, m
De	Dean number
f	friction factor
h	heat transfer coefficient, W/m^2K
k	thermal conductivity, W/mK
L	length of the tube, m
m	mass flow rate, kg/s
Nu	Nusselt number
Pr	Prandtl number
Re	Reynolds number
R_f	fouling factor, m^2K/W
U	overall heat transfer coefficient, W/m^2K
R	coefficient of determination
X	variable

Greek symbols

δ	curvature ratio
ΔP	pressure drop, kPa
ε	heat exchanger effectiveness, %
ν	kinematic viscosity, m^2/s
ρ	density, kg/m^3

Subscripts

i	inner
o	outer
s	surface
sh	shell
st	straight tube
targ	target

Acronyms

ANN	artificial neural network
HCT	helically coiled tube

HEX heat exchanger
HT heat transfer
HTC heat transfer coefficient
HVAC heating, ventilation and air conditioning
MAPE mean absolute percentage error, %
MLP multilayer perceptron
MoD margin of deviation
MSE mean squared error
NTU number of transfer unit
PD pressure drop
PEC performance evaluation criteria
RMSE root mean square error
SHCTHEX shell-helical coiled tube heat exchanger
STHEX shell and tube heat exchanger

References

[1] A.E. Bergles, Techniques to enhance heat transfer, in: W.M. Rohsenow, J.P. Hartnett, Y.I. Cho (Eds.), Handbook of Heat Transfer, McGraw-Hill, New York, 1998.
[2] H. Zhu, H. Wang, G. Kou, Experimental study on the heat transfer enhancement by Dean Vortices in spiral tubes, Int. J. Energy Environ. 5 (3) (2014) 317–326.
[3] D. Akgul, S.M. Kirkar, B.S. Onal, A. Celen, A.S. Dalkilic, S. Wongwises, Single-phase flow heat transfer characteristics in helically coiled tube heat exchangers, Kerntechnik 7 (1) (2022) 1–25.
[4] B.S. Onal, S.M. Kirkar, D. Akgul, A. Celen, O. Acikgoz, A.S. Dalkilic, S.N. Kazi, S. Wongwises, Heat transfer and pressure drop characteristics of two phase flow in helical coils, Therm. Sci. Eng. Prog. 27 (2022) 1–22, 101143.
[5] M. Mohanraj, S. Jayaraj, C. Muraleedharan, Applications of artificial neural networks for thermal analysis of heat exchangers - a review, Int. J. Therm. Sci. 90 (2015) 150–172.
[6] Z. Yang, Z.R. Yang, 'Artificial neural networks', in: A. Brahme (Ed.), Comprehensive Biomedical Physics, vol. 6, Elsevier, 2014, pp. 1–17.
[7] F. Marini, R. Bucci, A.L. Magri, A.D. Magri, Artificial neural networks in chemometrics: history, examples and perspectives, Microchem. J. 88 (2) (2008) 178–185.
[8] R. Beigzadeh, M. Rahimi, Prediction of heat transfer and flow characteristics in helically coiled tubes using artificial neural networks, Int. Commun. Heat Mass Tran. 39 (2012) 1279–1285.
[9] J. Cao, X. Wang, Y. Yuan, Z. Zhang, Y. Liu, Multi-objective optimization of micro-fin helical coil tubes based on the prediction of artificial neural networks and entropy generation theory, Case Stud. Therm. Eng. 28 (2021) 1–21.
[10] J. Gill, J. Singh, Use of artificial neural network approach for depicting mass flow rate of R134a/LPG refrigerant through straight and helical coiled adiabatic capillary tubes of vapor compression refrigeration system, Int. J. Refrig. 86 (2018) 228–238.
[11] M. Hajjat, Nanofluids as coolant in a shell and tube heat exchanger: ANN modeling and multi-objective optimization, Appl. Math. Comput. 365 (2020) 1–15.
[12] T.N. Verma, P. Nashine, D.V. Singh, T.S. Singh, D. Panwar, ANN: prediction of an experimental heat transfer analysis of concentric tube heat exchanger with corrugated inner tubes, Appl. Therm. Eng. 120 (2017) 219–227.
[13] J.D. Moya-Rico, A.E. Molina, J.F. Belmonte, J.I.C. Tendero, J.A. Almendros-Ibanez, Characterization of a triple concentric-tube heat exchanger with corrugated tubes using Artificial Neural Networks (ANN), Appl. Therm. Eng. 147 (2019) 1036–1046.
[14] A.N. Skrypnik, A.V. Shchelchkov, Y.F. Gortyshov, I.A. Popov, Artificial neural networks application on friction factor and heat transfer coefficients prediction in tubes with inner helical-finning, Appl. Therm. Eng. 206 (2022) 1–13.
[15] A.B. Colak, O. Acikgoz, H. Mercan, A.S. Dalkilic, S. Wongwises, Prediction of heat transfer coefficient, pressure drop, and overall cost of double-pipe heat exchangers using the artificial neural network, Case Stud. Therm. Eng. 39 (2022) 1–14.
[16] R.M. Devi, P. Murugesan, M. Venkatesan, P. Keerthika, K. Sudha, J.C. Kannan, P. Suresh, Development of MLP-ANN model to predict the Nusselt number of plain swirl tapes fixed in a counter flow heat exchanger, Mater. Today Proc. 46 (2021) 8854–8857.
[17] Z. Said, S. Rahman, P. Sharma, A.A. Hachicha, S. Issa, Performance characterization of a solar-powered shell and tube heat exchanger utilizing MWCNTs/water-based nanofluids: an experimental, numerical, and artificial intelligence approach, Appl. Therm. Eng. 212 (2022) 1–16.
[18] D. Akgul, D. Mercan, A.S. Dalkilic, Parametric optimization of heat transfer characteristics for helical coils, J. Therm. Anal. Calorim. 147 (7) (2022) 12577–12594.
[19] Y.A. Cengel, Heat Transfer - A Practical Approach, second ed., McGraw-Hill, 2002.
[20] W.R. Dean, XVI. Note on the motion of fluid in a curved pipe, Philosophical Magazine, Series 7 4 (20) (1927) 208–223.
[21] A.N. Dravid, K.A. Smith, E.W. Merrill, P.L.T.(Brian, Effect of secondary fluid motion on laminar flow heat transfer in helically coiled tubes, American Institute of Chemical Engineers Journal 17 (5) (1971) 1114–1122.
[22] R.K. Shah, D.P.(Sekulic, Fundamentals of Heat Exchanger Design, John Wiley & Sons, 2003.
[23] C.H. Forsberg, Heat Transfer Principles and Applications, Academic Press, 2020.
[24] C.M. White, Streamline flow through curved pipes, Proceedings of the Royal Society of London, Series A 123 (1929) 645–663.
[25] R.L. Webb, Performance evaluation criteria for use of enhanced heat transfer surfaces in heat exchanger design, Int. J. Heat Mass Tran. 24 (4) (1981) 715–726.
[26] W.T. Ji, J.F. Fan, C.Y. Zhao, W.Q. Tao, A revised performance evaluation method for energy saving effectiveness of heat transfer enhancement techniques, Int. J. Heat Mass Tran. 138 (2019) 1142–1153.
[27] H. Mercan, F. Sonmez, A.B. Colak, A.S. Dalkilic, Determination of heat transfer rates of heavy-duty radiators for trucks having flattened and double-U grooved pipes with louvered fins by ANN method: an experimental study, The European Physical Journal Plus 137 (2022) 1–26.
[28] T. Calisir, A.B. Colak, D. Aydin, A.S. Dalkilic, S. Baskaya, Artificial neural network approach for investigating the impact of convector design parameters on the heat transfer and total weight of panel radiators, Int. J. Therm. Sci. 183 (2023) 1–12.
[29] A.B. Colak, A. Celen, A.S. Dalkilic, Numerical determination of condensation pressure drop of various refrigerants in smooth and micro-fin tubes via ANN method, Kerntechnik 87 (5) (2022) 506–519.
[30] O. Kalkan, A.B. Colak, A. Celen, K. Bakirci, A.S. Dalkilic, Prediction of experimental thermal performance of new designed cold plate for electric vehicles' Li-ion pouch-type battery with artificial neural network, J. Energy Storage 48 (2022) 1–12.